INFRARED DETECTION OF FOREST FIRES FROM SPACE UNDER CONDITIONS OF A CLOUDY ATMOSPHERE

V.G. Astafurov and G.A. Titov

Institute of Atmospheric Optics,
Siberian Branch of the Russian Academy of Sciences, Tomsk
Received January 31, 1996

The feasibilities are explored for detection of seats of forest fires using spectral infrared radiation measurements under conditions of cumulus clouds from space. This problem is solved by a statistical hypothesis testing method. A decision rule is based on the Neumann–Pearson test. Statistical models of signal (the fire seat emission) and background (the radiation from the underlying surface, clouds, and the atmosphere) have been proposed and validated. Analysis of the results obtained shows the feasibility of reliable detection of forest fires over an area of about 600 m^2 *provided that the cloud amount does not exceed* 0.5.

INTRODUCTION

At present remote sensing techniques provide powerful means for studying the atmosphere from meteorological satellites using thermal infrared (IR) radiation measurements. These techniques make possible determination of the underlying surface temperature as well as detection of areas with elevated temperature, i.e., seats of forest fires. A search for the forest fires and their detection in incipient stage are of primary interest to decrease essentially the number of heavy fires and to reduce expenses on fire control.

Available algorithms for detecting forest fires are based on the IR radiation measurements in the spectral ranges from 3.55 to 3.93 μm and from 10.3 to 11.3 μm lying in the atmospheric windows.[1] For temperatures typical of forest fires ranging from 800 to 1000 K the radiation maximum is in the first spectral range. The radiation maximum of the underlying surface at a temperature of 300 K is in the second spectral range. Such spectral channels are available in the AVHRR radiometers placed on board the NOAA meteorological satellites. As shown in Ref. 1, infrared radiation measurements with 1-km^2 resolution permit detection of the seats of forest fires at $T \sim 1000$ K over an area of 100 m^2 as well as zones of smouldering at $T \sim 600$ K over an area of 900 m^2. The presence of cloudiness essentially limits the possibilities of existing techniques for IR detecting the forest fires.

This paper considers a problem of detection of the forest fires under conditions of cumulus clouds as a statistical hypothesis testing problem. Such an approach is connected with the presence of breaks in the cloud field and partial transmission of radiation of the seats of forest fires (SFF) through optically thin clouds or their edges. The last circumstance leads to essential enlargement of the area of possible detection of SFF. The problem is solved under conditions of significant fluctuations of the measurable radiative temperature because of the clouds fall within a radiometer view.

CRITERION OF DETECTION

A decision rule for detecting SFF can be formulated using different criteria, namely, Bayesian, maximum *a posteriori* probability, maximum likelihood, and Neuman–Pearson criteria.[2] Selection of the criterion depends on the available *a priori* statistical data, i.e., the probability q that SFF falls within the radiometer view and the probability density $f(P(\Delta\lambda_1), P(\Delta\lambda_2))$ of powers $P(\Delta\lambda_i)$ radiated by SFF in spectral ranges $\Delta\lambda_i$, $i = 1, 2$. Decision rules formulated by different criteria will be distinguished not only by decision algorithms but also by their quality.

Let us accept two hypotheses: H_0 that SFF is absent in the receiver view and H_1 that SFF is in the receiver view. When the hypothesis H_0 is true, the receiver records only the background radiation of the underlying surface, clouds, and the atmosphere and when the hypothesis H_1 is true, the background and the signal taken to mean the SFF radiation are recorded. Because of the presence of the signal and background fluctuations due to the radiative transfer through the cumulus clouds, the errors of two types are possible:

1) The decision γ_1 is taken on the presence of SFF while the hypothesis H_0 is true, namely, only the background is detected. This error is characterized by the conditional probability $\alpha = P(\gamma_1 | H_0)$. Further α will be called the probability of false alarm.

2) The decision γ_0 is taken on the absence of SFF in the detector view while the hypothesis H_1 is true, i.e., the receiver records the radiation of the fire seat and the background. This error is of the second type with the conditional probability $\beta = P(\gamma_0 | H_1)$. The conditional

0235-6880/96/05 409-06 $02.00

probability of true detection $P(\gamma_1|H_1)$ complements β to unity, i.e., $P(\gamma_1|H_1) = 1 - \beta$.

We introduce the following designations: $\mathbf{p}(\theta_0) = (p_1(\theta_0), p_2(\theta_0))$ is the vector of powers $p_i(\theta_0)$ recorded by the IR-radiometer at altitude h_0 in the spectral ranges $\Delta\lambda_i$ (θ_0 is the zenith angle of observation); $f(\mathbf{p}(\theta_0)|H_0) = f_0(\mathbf{p})$ and $f(\mathbf{p}(\theta_0)|H_1) = f_1(\mathbf{p})$ are the joint conditional probability densities of the vector of sampling data in the hypotheses H_0 and H_1, respectively. A set of values $\mathbf{p}(\theta_0)$ forms a space of sampling data E_2. To formulate the decision rule by any criterion, the probability densities $f_0(\mathbf{p})$ and $f_1(\mathbf{p})$ are necessary, first of all, to write the likelihood ratio. The *a priori* probability q and the *a priori* probability density $f(P(\Delta\lambda_1), P(\Delta\lambda_2))$ are required for the Bayes criterion, the *a posteriori* probability maximum criterion, and the maximum likelihood criterion.

If the Bayes criterion is used, which minimizes the mean risk, the information for setting the loss function is also necessary. This information specifies the charge for the errors of the first and second types. We have no information for validated assignment of the loss function, the probability q, and the probability density $f(P(\Delta\lambda_1), P(\Delta\lambda_2))$. Under these conditions, it is feasible to use the Neumann–Pearson criterion.[2] This criterion makes it possible to formulate the decision rule, providing the maximum probability of true detection $1 - \beta$ at a given probability of false alarm α. The decision rule based on the selected criterion specifies the probability ratio

$$\Lambda(\mathbf{p}(\theta_0)) = \frac{f_1(\mathbf{p})}{f_0(\mathbf{p})}$$

and compares it with the threshold u_α, whose value for the Neumann–Pearson criterion is determined from the condition

$$P\{\Lambda(\mathbf{p}(\theta_0))|P(\Delta\lambda_i) = 0,\ i = 1,\ 2\} = \alpha.$$

In this case, the sample space E_2 will be divided into two non-overlapping regions G_0 and G_1 corresponding to the decision γ_0 if $\mathbf{p}(\theta_0) \in G_0$ or γ_1, if $\mathbf{p}(\theta_0) \in G_1$. Thus, to formulate the decision rule within the scope of the selected parametric approach to the solution of the SFF detection problem, we must study the joint statistical characteristics of powers $p_1(\theta_0)$ and $p_2(\theta_0)$.

This paper consideres the SFF detection based on the IR-radiation measurements in one spectral range $\Delta\lambda_i$. Such an approach can be considered as the first stage of solution of the above-mentioned problem, enabling one to estimate the feasibilities of SFF detection under conditions of cumulus clouds. In this case, the initial information for arriving at the decision is the radiative power $p = p_i(\theta_0)$ recorded with a radiometer in one of the spectral intervals $\Delta\lambda_i$. Since the mean values of p in the hypotheses H_0 and H_1 satisfy the evident condition $\langle p\rangle_1 > \langle p\rangle_0$, then the entire interval of possible values of p is divided by the threshold u_α into two intervals[2] $[0, u_\alpha]$ and $(u_\alpha, +\infty)$. Decisions are taken by the following rule: γ_0 (SFF is absent) if $p \in [0, u_\alpha]$ and γ_1 (SFF is present) if $p \in (u_\alpha, +\infty)$. The value of threshold is obtained from the equation

$$\alpha = \int_{u_\alpha}^{+\infty} f_0(p)\mathrm{d}p, \qquad (1)$$

and the probability of true detection equals

$$1 - \beta = \int_{u_\alpha}^{+\infty} f_1(p)\mathrm{d}p. \qquad (2)$$

The distribution $f_0(p)$ is determined only by the statistical characteristics of the background and does not depend on the SFF radiation power $P(\Delta\lambda_i)$ in the selected spectral interval $\Delta\lambda_i$.

STATISTICAL MODELS OF SIGNAL AND BACKGROUND

Selection of approximations for the probability densities $f_j(p)$ ($j = 0,1$) is the most important stage of the detection problem solution. This is explained by the fact that the threshold value u_α depends significantly on the behavior of $f_0(p)$ at large values of p, i.e., at "tails" of the distribution. The behavior of $f_0(p)$ at the tails is determined by the distribution moments of order higher than the variance. Therefore, to select the qualitative approximation for the probability densities $f_j(p)$ ($j = 0,1$), for example, according to the Pearson curves,[3] we must know the first four moments of power p.

For analytical setting of the probability densities $f_j(p)$, we can use their series expansion in orthogonal polynomials. Since $f_j(p) = 0$ for $p < 0$, then the approximation by the Laguerre series

$$f_j(p) = \sum_{n=0}^{\infty} c_{j,n} \mathrm{e}^{-p} p^{\nu_j} L_n^{(\nu_j)}(p),\ \ j = 0,\ 1, \qquad (3)$$

is suitable,[3] where $L_n^{(\nu_j)}(p)$ is the generalized Laguerre polynomial and $c_{j,n}$ are the expansion coefficients. To determine the nth expansion coefficient $c_{j,n}$, we must know the first n initial moments $\langle p^n\rangle$. Therefore, the number of terms of series (3) is determined by the number of known moments $\langle p^n\rangle$. If we know the average and the variance, then Eq. (3) coincides with the gamma distribution

$$f_j(p) = \frac{1}{\eta_j\,\Gamma(\nu_j + 1)} \left(\frac{p}{\eta_j}\right)^{\nu_j} \exp\left(-\frac{p}{\eta_j}\right), \qquad (4)$$

whose parameters are determined by the formulas

$$\nu_j = \frac{\langle p \rangle_j^2}{D_j(p)} - 1, \quad \eta_j = \frac{D_j(p)}{\langle p \rangle_j}, \quad j = 0,1. \tag{5}$$

To evaluate the accuracy of approximation of Eq. (4), we must consider the term corresponding to $n = 3$ in Eq. (3). In this case, the following expression

$$f_j(p) = \frac{1}{\eta_j}\left(\frac{p}{\eta_j}\right)^{\nu_j} \exp\left(-\frac{p}{\eta_j}\right)\left(\frac{1}{\Gamma(\nu_j + 1)} + c_{j,3}\, L_3^{(\nu_j)}\left(\frac{p}{\eta_j}\right)\right) \tag{6}$$

is valid, where

$$L_3^{(\nu_j)}(p) = [(\nu_j + 1)(\nu_j + 2)(\nu_j + 3) -$$

$$- 3p(\nu_j + 2)(\nu_j + 3) + 3p^2(\nu_j + 3) - p^3]/6,$$

$$c_{j,3} = \frac{(\nu_j + 1)(\nu_j + 2)(\nu_j + 3)}{\Gamma(\nu_j + 4)}\,(1 - \xi_{\gamma,j}), \tag{7}$$

$$\xi_{\gamma,j} = \langle p^3 \rangle_j / \langle p^3 \rangle_j^{(\gamma)} \tag{8}$$

is the ratio of $\langle p^3 \rangle_j$ to the third moment

$$\langle p^3 \rangle_j^{(\gamma)} = \eta_j^3(\nu_j + 1)(\nu_j + 2)(\nu_j + 3) \tag{9}$$

of the gamma distribution p. The difference $1 - \xi_{\gamma,j}$ in Eq. (7) characterizes the relative deviation of the third moments $\langle p^3 \rangle_j$ and $\langle p^3 \rangle_j^{(\gamma)}$. Therefore, the deviation of $\xi_{\gamma,j}$ from unity can be considered as the degree of accuracy of $f_j(p)$ approximation by the gamma-distribution at the level of the third moments.

SOLUTION TECHNIQUE

To determine the threshold u_α and to calculate the probability of true detection $1 - \beta$, approximation (4) or (6) is proposed for $f_j(p)$ depending on the value of the parameter $\xi_{\gamma,j}$ determined by Eq. (8). The moments of thermal radiation power in the selected spectral ranges $\Delta\lambda_i$, $i = 1, 2$, are calculated using the numerical simulation technique. The recorded power is determined by the expression

$$p_i(\theta_0) = \int_{\Delta\Omega} d\boldsymbol{\omega} \int_{S_R^*} d\boldsymbol{\rho} \int_{\Delta\lambda_i} d\lambda k(\lambda) I(\boldsymbol{\rho}, \boldsymbol{\omega}, \lambda), \tag{10}$$

where S_R^* is the aperture of the receiving antenna of area S_R, $\Delta\Omega$ is the field–of–view angle of the radiometer, $k(\lambda)$ is the transmission coefficient of an optical filter at the wavelength λ, and $I(\boldsymbol{\rho}, \boldsymbol{\omega}, \lambda)$ is the intensity of upwelling thermal radiation at a point $\boldsymbol{\rho} \in S_R^*$ in the direction of unit vector $\boldsymbol{\omega}$.

To calculate the intensity of upwelling IR radiation, we consider the nonscattering atmosphere being in the state of local thermodynamic equilibrium, horizontally homogeneous (except for a cloud layer, whose lower boundary is located at the altitude h_b), with the temperature $T(z)$ at the altitude z and the aerosol and gaseous extinction coefficient $\alpha(z, \lambda)$. Within the cloud layer the total extinction coefficient at the altitude z equals $\alpha_\Sigma(z, \lambda) = \alpha(z, \lambda) + \alpha_\Gamma(\lambda)\chi(\mathbf{r})$, and $\chi(\mathbf{r})$ is the indicator field

$$\chi(\mathbf{r}) = 1 \text{ if } \mathbf{r} \in \Theta \text{ and } \chi(\mathbf{r}) = 0 \text{ if } \mathbf{r} \notin \Theta,$$

where Θ is a random set of points in which the cloud substance with the extinction coefficient $\alpha_\Gamma(\lambda)$ is present. We consider the underlying surface to be an ideal black-body emitter with the temperature distribution $T_s(x, y)$ and the clouds are nonscattering media. The accuracy of the latter approximation when calculating the long-wave radiation flux in the presence of cumulus clouds was considered in detail in Ref. 4. Based on the above assumptions, the intensity of upwelling thermal radiation at altitude h_0 is determined by the well–known expression

$$I(\boldsymbol{\rho},\boldsymbol{\omega},\lambda) = B_\lambda(T_s(x, y))\exp\left(-\frac{1}{\mu}\int_0^{h_0} \alpha_\Sigma(s, \lambda)ds\right) +$$

$$+ \int_0^{h_0} B_\lambda(T(z))\exp\left(-\frac{1}{\mu}\int_z^{h_0} \alpha_\Sigma(s, \lambda)ds\right)\frac{\alpha_\Sigma(z, \lambda)}{\mu}\,dz, \tag{11}$$

where $B(T_s)$ is the Planck function, $\mu = \cos\theta_0$, $x = x(\boldsymbol{\omega}, h_0)$, and $y = y(\boldsymbol{\omega}, h_0)$. The first term in Eq. (11) is the radiation of the underlying surface transformed by the atmosphere and the second term is the radiation of the atmosphere.

The estimates of the power moments p are calculated by the successive simulation of realizations of the cloud field, calculation by formula (11) of the intensity of upwelling thermal radiation for each direction being in the receiver view, calculation of the power p by formula (10), and subsequent averaging over realizations of the cloud field.

Simulation of realizations of the cloud field was considered in detail in Ref. 5. It is assumed that a separate cloud is of the form of a truncated paraboloid, whose diameter D is equal to its height and has an exponential distribution $f(D) \sim \exp(-\alpha D)$, $\alpha = 2.30 < D < 1300$ m. The altitude of the lower boundary of the cloud layer equals 1 km. The extinction coefficient $\alpha_\Gamma(\lambda)$ is for C1 cloud[6] at wavelengths of 4 and 10 μm. Since the scattering effects are not taken into account, the realizations of the cloud field are simulated only within the radiometer view. Then it is divided into square cells. Each cell is 25 m in horizontal size. For each cell the thickness of the cloud layer is calculated. In our calculations, we used the vertical profiles of the aerosol extinction coefficient borrowed from Ref. 7. The profiles of the humidity and temperature for the summer atmospheric model at mid-latitudes were borrowed from Ref. 8. The water vapor absorption for the selected spectral ranges was considered using the technique described in Ref. 9. In calculations of the

intensity $I(\boldsymbol{\rho}, \boldsymbol{\omega}, \lambda)$ and the power p we used the methods of numerical integration over the altitude z, the spectral range $\Delta\lambda_i$, and the field–of–view angle $\Delta\Omega$ of the radiometer.

RESULTS OF CALCULATION

In general the distribution of T_s over the SFF is very complicated and is determined by a large number of different factors.[10] The principal purpose of this paper is to illustrate the feasibility of detection of the seats of forest fires under conditions of cumulus clouds. Therefore, in our calculations the simplest model of SFF is used consisting of two temperature zones, i.e., the zone of smouldering with T = 600 K and the seat of fire with T_s = 1000 K.

Figure 1 shows an example of realization of the intensity field of upwelling thermal radiation $\int_{\Delta\lambda_i} I(\boldsymbol{\rho}, \boldsymbol{\omega}_\perp, \lambda)d\lambda$ at the upper boundary of the atmosphere in spectral ranges from 3.55 to 3.93 μm and from 10.3 to 11.3 μm for the cloud amount N = 0.5, and $\boldsymbol{\omega}_\perp$ = (0; 0; 1). The seat of fire represents two bands parallel to the OX axis: the first band at T_s = 600 K is extended at $0.53 \le y \le 0.58$ km and the second band at T_s = 1000 K is extended at $0.58 < y \le 0.68$ km. The temperature of the other zones is 300 K. Figure 1 shows different temperature zones, which are not anywhere resolved within the band of the fire seat. This is explained by significant difference in the radiation intensities for the regions of the underlying surface with different temperatures. The figure illustrates the visibility of different zones of the seat of fire overcast with optically thin clouds or their edges. For the given realization of the cloud field, only one region of the fire seat is not visible overcast with optically thick central part of a cloud about 800 m in diameter.

All subsequent calculations were carried out for h_0 = 850 km, the field–of–view angle $\Omega = 1.88 \cdot 10^{-6}$ sr and $\Theta = 0$ (the nadir direction). In this case, the area of the underlying surface S, falling within the radiometer view, equals 1 km^2. The relative dimensions of zones of the fire seat are determined by the two parameters:

$$d_1 = \Delta S(T_s = 1000 \text{ K})/S,$$

$$d_2 = \Delta S(T_s = 600 \text{ K})/S,$$

where $\Delta S(T_s)$ is the area of the surface region at temperature T_s falling within the radiometer view. Figures 2 and 3 show the results of calculation of the curves of the dependence of relative moments of the power p recorded by the radiometer (here, $\delta = \sqrt{D(p)}/\langle p \rangle$ is the relative standard deviation and $k_\gamma = M_3(p)/D^{3/2}(p)$ is the asymmetry coefficient) on the cloud amount N for different values of the parameters d_1 and d_2. At $d_1 = d_2 = 0$, the temperature of the whole region of the underlying surface equals 300 K that corresponds to the absence of SFF in the receiver view.

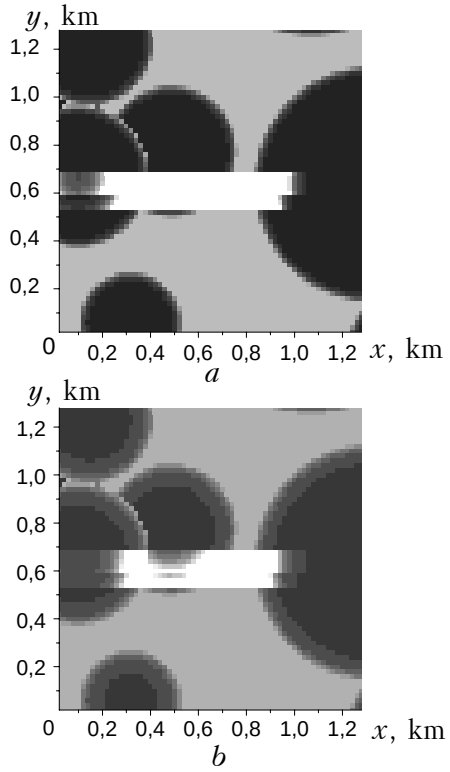

FIG. 1. Realization of the intensity field of upwelling thermal radiation in the spectral ranges from 3.55 *to* 3.93 μm *(a) and from* 10.3 *to* 11.3 μm *(b) for the cloud amount* N = 0.5 *(brightness is proportional to the value of the intensity).*

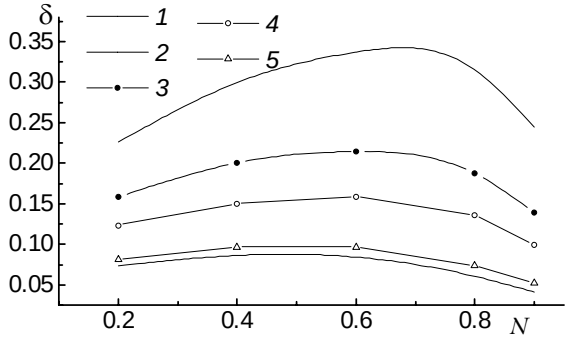

FIG. 2. Dependence of the relative standard deviation δ *of the power* p *on the cloud amount* N *for the spectral range from* 10.3 *to* 11.3 μm: d_1 = 0 *(1),* 0.0025 *(3, 4, and 5), and* 0.01 *(2);* d_2 = 0 *(1 and 5),* 0.024 *(4),* 0.05 *(3), and* 0.1 *(2).*

The most important results are the calculated coefficients ξ_γ, determined by Eq. (8) and characterizing the degree of deviation of the probability density $f_j(p)$, determined by Eq. (6), from gamma distribution given by Eq. (4). The curves of the dependence of ξ_γ on N are shown in

Fig. 4. The parameters ν and η were calculated by formulas (5). The figure shows that the value of ξ_γ is close to unity in the absence of the fire seat. The presence of SFF in the radiometer view results in the deviation of ξ_γ from unity. The magnitude of this deviation in the first channel is much larger than in the second channel. In this case, the dependence of ξ_γ on the fire seat area is nonmonotonic. From the above-said it follows that for determining the threshold u_α in Eq. (1), the gamma distribution can be used for the approximation of $f_0(p)$ with a large degree of accuracy.

Probabilities of detection of the fire seats of different size are shown in Fig. 5. The results of calculations indicate that the detection efficiency in the first spectral range is much higher than in the second range. As indicated above, this is explained by the fact that in this range the radiation maximum occurs at temperatures of about 1000 K. Figure 5*a* shows that the probability of SFF detection of size 25×25 m in the first spectral range for $N < 0.5$ is sufficiently high: $1 - \beta > 0.8$. However, it should be noted that the probability of true detection for the spectral range from 3.55 to 3.93 μm is determined neglecting the interference of backscattering due to the reflected solar radiation. It can be large, especially in the presence of cumulus clouds or strongly reflecting vegetation.[11] In the second spectral range this interference is absent.

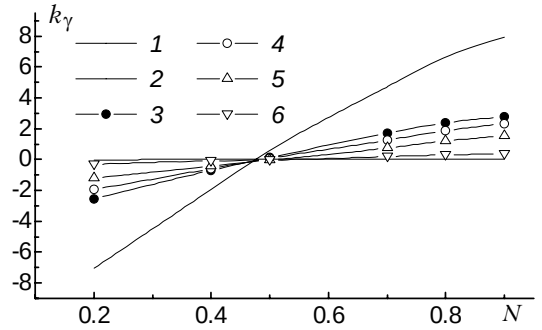

FIG. 3. Dependence of the asymmetry coefficient k_γ of the power p on the cloud amount N for the spectral range from 3.55 *to* 3.93 μm: $d_1 = 0$ *(1),* 0.000625 *(6),* 0.0025 *(3, 4, and 5), and* 0.01 *(2); $d_2 = 0$ (1, 5, and 6),* 0.024 *(4),* 0.05 *(3), and* 0.1 *(2).*

The results obtained indicate a principal feasibility of detection of the seats of forest fires under conditions of cumulus clouds. To increase the detection efficiency, one must develop the algorithms using the results of measurements of a two-channel receiver that will enable one to consider different temperature dependence of the background and the seat of the fire in different spectral ranges.

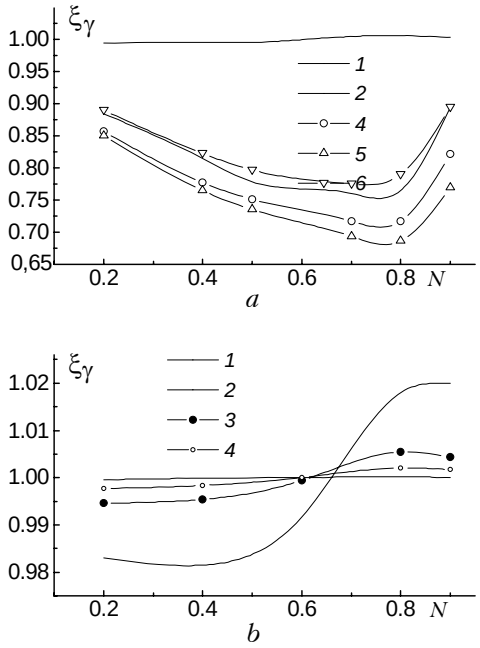

FIG. 4. Dependence of ξ_γ on the cloud amount N for spectral ranges from 3.55 to 3.93 μm *(a) and from* 10.3 *to* 11.3 μm *(b). Designations are the same as in Fig. 3.*

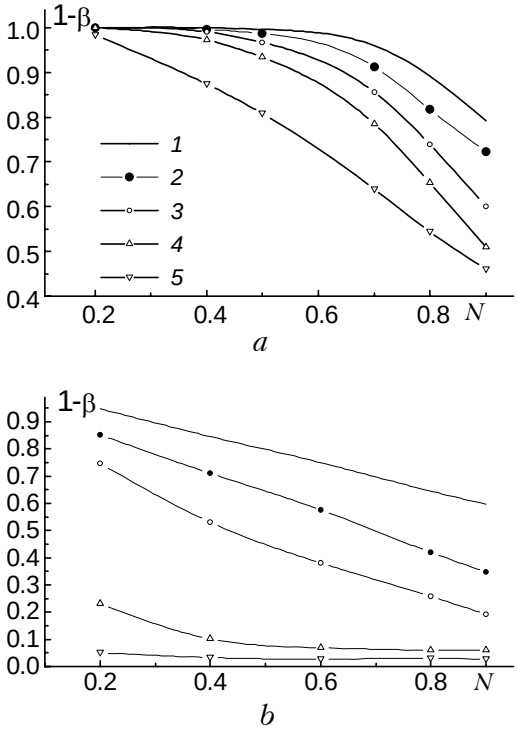

FIG. 5. Dependence of the probability of true detection of the seat of fire $1 - \beta$ *on the cloud amount N at* $\alpha = 0.02$ *for spectral ranges from* 3.55 *to* 3.93 μm *(a) and from* 10.3 *to* 11.3 μm *(b): $d_1 = 0.000625$ (5),* 0.0025 *(2, 3, and 4), and* 0.01 (1); *$d_2 = 0$ (4 and 5),* 0.024 *(3),* 0.05 *(2), and* 0.1 *(1).*

REFERENCES

1. Y.J. Kaufman and C.J. Tucker, J. Geophys. Res. **95**, No. D7, 9927–9939 (1990).
2. B.R. Levin, *Theoretical Fundamentals of Statistical Radio Engineering* (Sov. Radio, Moscow, 1968), Vol. 2, 503 pp.
3. V.I. Tikhonov, *Statistical Radio Engineering* (Radio i Svyaz', Moscow, 1982), 624 pp.
4. E.I. Kas'yanov and G.A. Titov, Atm. Opt. **2**, No. 2, 102–108 (1989).
5. V.E. Zuev and G.A. Titov, Atmos. Oceanic Opt. **8**, Nos. 1–2, 105–115 (1995).
6. D. Deirmendjian, *Electromagnetic Scattering on Spherical Polydispersions* (Elsevier, Amsterdam; American Elsevier, New York, 1969).
7. V.E. Zuev and G.M. Krekov, *Optical Models of the Atmosphere* (Gidrometeoizdat, Leningrad, 1986), 256 pp.
8. V.E. Zuev and V.S. Komarov, *Statistical Models of the Temperature and Gaseous Components of the Atmosphere* (D. Reidel Publishing Company, Dordrecht/Boston/Lancaster/Tokyo, 1987).
9. M.E. Thomas and C.T. Delaye, in: *Proceedings of the 14th Conference on Atmospheric Transmission Models,* Massachusetts (1991), pp. 342–349.
10. A.M. Grishin, *Mathematical Simulation of Forest Fires: New Methods of Fighting with the Forest Fires* (Nauka, Novosibirsk, 1992), 407 pp.
11. M.S. Malkevich, *Optical Studies of the Atmosphere Using Satellites* (Nauka, Moscow, 1973), 303 pp.